

Robustness of traveling states in generic nonreciprocal mixturesRituparno Mandal ^{1,2,*}, Santiago Salazar Jaramillo ¹ and Peter Sollich^{1,3,†}¹*Institute for Theoretical Physics, Georg-August-Universität Göttingen, 37077 Göttingen, Germany*²*James Franck Institute, The University of Chicago, Chicago, Illinois 60637, USA*³*Department of Mathematics, King's College London, London WC2R 2LS, United Kingdom*

(Received 2 January 2023; revised 11 February 2024; accepted 26 April 2024; published 5 June 2024)

Emergent nonreciprocal interactions violating Newton's third law are widespread in out-of-equilibrium systems. Phase separating mixtures with such interactions exhibit traveling states with no equilibrium counterpart. Using extensive Brownian dynamics simulations, we investigate the existence and stability of such traveling states in a generic nonreciprocal particle system. By varying a broad range of parameters including aggregate state of mixture components, diffusivity, degree of nonreciprocity, effective spatial dimension and density, we determine that traveling states do exist below the predator-prey regime, but nonetheless are only found in a narrow region of the parameter space. Our work also sheds light on the physical mechanisms for the disappearance of traveling states when relevant parameters are being varied, and has implications for a range of nonequilibrium systems including nonreciprocal phase separating mixtures, nonequilibrium pattern formation and predator-prey models.

DOI: [10.1103/PhysRevE.109.L062602](https://doi.org/10.1103/PhysRevE.109.L062602)

Introduction. Fundamental pairwise interactions such as gravitational or electromagnetic forces always obey action-reaction symmetry. This is also true for effective pairwise interactions between particles in an equilibrium medium like the Asakura-Oosawa attraction [1] between colloidal particles in a medium of nonadsorbing macromolecules. Similar examples arise in the context of Casimir forces between compact objects [2]. This paradigm can break down if either the medium or the interacting particles are driven out of equilibrium [3], resulting in nonreciprocal interactions [4,5]; these have generated very substantial interest in the last decade [6–23].

A striking observation is that nonreciprocal systems can give rise to exotic time-dependent steady states [15,16,18,22] with stable traveling waves. Although hydrodynamic continuum descriptions [15,16,18,24–29] have shed some light on the conditions under which traveling states arise and their stability with respect to changes in material parameters, similar insights from particle-based models remain scarce. One instance is a study of particles with long-ranged nonreciprocal diffusiophoretic interactions mediated by concentration gradients in the surrounding medium [22] and another involves quorum sensing in active matter [30].

Here we explore a generic particle-based model of a nonreciprocal system with short-ranged interactions, employing Brownian dynamics simulations to investigate the existence and stability of collective traveling states. The particle-based approach implements nonreciprocal interactions directly at

the microscopic level, unlike in hydrodynamic models where nonreciprocal effects have to be included via coarse graining which, with rare exceptions [31], cannot be done exactly. We systematically vary the most relevant parameters that potentially influence traveling states, such as the diffusivity D_0 and density of the constituent particles ρ , the aggregate state (gas, liquid, solid) of the mixture components, the degree of nonreciprocity δ , and the degree of confinement and with it the effective spatial dimension. We identify the physical mechanisms that maintain or destroy traveling states, and find that the requirements for such states are met only in a narrow region of the parameter space.

Model. We study a binary mixture of species A and B (see the Supplemental Material [32], for details on the model and numerical solution) in two dimensions with Lennard-Jones (LJ) interactions, with homogeneously mixed initial conditions unless stated otherwise. The intraspecies (AA or BB) interaction is reciprocal; we tune the strength of its attractive part to make the individual components of the mixture (A or B), in pure form and in equilibrium at low temperature, behave as a gas, liquid, or solid. When phase separation occurs in the combined (50% A, 50% B) system, we find that the A- and B-rich phases then also have gas, liquid and solidlike features, and label them accordingly. For the interspecies (AB, BA) interaction we take the repulsive part ($\sim 1/r^{12}$) as reciprocal, thus defining the physical core size of the particles. The attractive part ($\sim 1/r^6$) is nonreciprocal, with a prefactor $1 \pm \delta$ where δ is the nonreciprocity parameter. For $\delta > 0$ there exists a stronger attractive force on A particles (colored blue in plots) from neighboring B particles (colored red) than on Bs from surrounding As. We focus on the range $0 < \delta < 1$ but have also explored the predator-prey regime of larger δ , e.g., $\delta \sim 1.5$, finding similar conclusions. We set the overall strength of the AB and BA attraction such that phase separation between

*rituparno.mandal@uni-goettingen.de

†peter.sollich@uni-goettingen.de

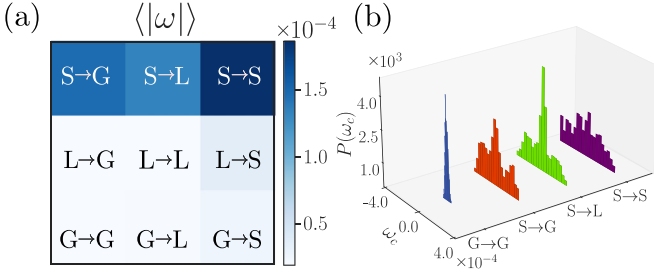


FIG. 1. (a) Mean angular velocity in annular geometry (with $R_{\text{in}} = 33$ and $R_{\text{out}} = 42$) for all combinations of aggregate states Solid, Liquid, and Gas, e.g., for A in solid and B in gas state we use $V_{AA} = 1$, $V_{BB} = 0$; see main text and SM [32] for details. The arrow indicates which species has the higher attraction toward the other species and will therefore tend to follow it as the “chasing cluster” in a traveling state. We use density $\rho = 0.1$, diffusivity $D_0 = 10^{-2}$, and $\delta = \pm 0.9$. (b) Probability distribution of center of mass angular velocity ω_c , for four combinations of aggregate states as indicated. Note the clearly visible peaks at nonzero ω_c for S → G. The distribution for G → G has been scaled down by a factor of four for better visualization.

A- and B-rich phases can occur, which is a precondition for traveling states.

We implement both periodic boundary conditions (PBC) [32], with a square box of linear size $L = 42$ and confined annular geometries (see the SM [32] for the advantages of this choice). To explore whether analogs of the traveling states found in hydrodynamic models [15,16,18] exist in our particle-based setup, we measure the average rotational velocity $\langle |\omega| \rangle$ (for annular geometry) or average translational velocity $\langle |\mathbf{v}| \rangle$ (in PBC or effectively $2d$ geometries), with

the average $\langle \dots \rangle$ being taken across all particles. We also analyze $P(\omega_c)$ or $P(v_c)$ (where ω_c and v_c are the angular and translational velocity of the center of mass) as a diagnostic: a probability peak at nonzero ω_c or v_c indicates a traveling state in the annular geometry or with PBC, respectively. The samples for these distributions are collected both across time in steady state and across the ensemble of trajectories [32].

Effects of aggregate state of mixture components. Physically, the aggregate state of each mixture component should be key in the emergence of traveling states. We therefore tune the intraspecies attraction strengths V_{AA} and V_{BB} such that the pure species A and B at equilibrium at low diffusivity (see below) are in a gas, liquid, or solid state [32]. In Fig. 1(a) we show the behavior for the nine resulting combinations for an annular geometry; for typical configurations see Fig. 2(b) and Fig. S1 [32]. A traveling state where the chasing cluster achieves a reasonable velocity appears only when the chasing particles have strong interparticle attractions. The same conclusion turns out to hold for other boundary conditions, e.g., PBC (see Fig. S2 [32]). The distribution of the center of mass angular velocity is generally broad when the chasing particles are in a solid state. Characteristic velocity peaks appear only when a solid cluster is chasing a gas [Fig. 1(b)], making this combination the most promising candidate for traveling states. This observation also holds in the predator-prey regime $\delta > 1$ and for larger system sizes (see Fig. S8 and Fig. S10 [32]). We therefore adopt the corresponding interaction strengths ($V_{AA} = 1$, $V_{BB} = 0$) for the rest of the analysis.

Effects of diffusivity and degree of nonreciprocity. Diffusivity, which plays the role of thermal fluctuations provided by the embedding medium, is another crucial factor in the collective dynamics. Figure 2(a) shows that the mean angular velocity of a nonreciprocal mixture generally decreases with

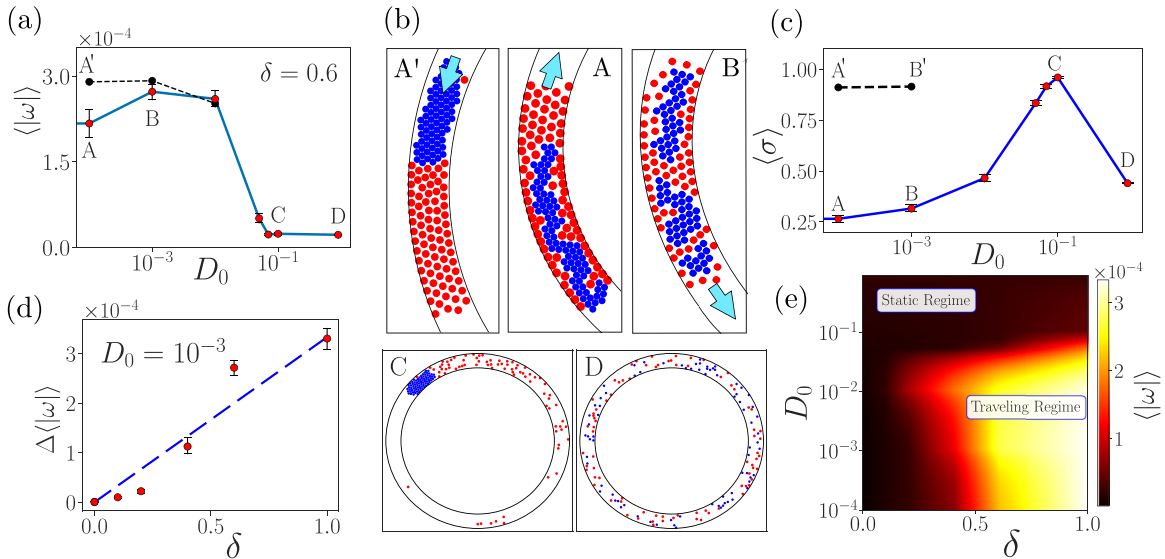


FIG. 2. Effects of diffusivity and nonreciprocity, for a system with the same density and annular geometry as in Fig. 1. (a) Average absolute angular velocity $\langle |\omega| \rangle$ of the particles plotted against diffusivity D_0 , for a system with $\delta = 0.6$ initialized in a phase separated state (dashed line and black filled circles) and for a mixed initial condition (solid blue line with red filled circles). (b) Snapshots of the binary mixture (direction of motion in the traveling cases is marked by arrows) for different D_0 and initial conditions as marked in (a). (c) Phase segregation order parameter $\langle \sigma \rangle$ [32] as a function of D_0 for mixed and segregated initial conditions [color scheme and $\delta = 0.6$ as in (a)]. (d) Dependence of net mean angular velocity $\Delta \langle |\omega| \rangle$ (see text for definition) on nonreciprocity parameter δ for $D_0 = 10^{-3}$. (e) Phase diagram from heat map of $\langle |\omega| \rangle$ against diffusivity D_0 and nonreciprocity parameter δ : traveling states appear when nonreciprocity is high and diffusivity is sufficiently low.

increasing diffusivity D_0 . To understand this, one has to bear in mind that the actual aggregate state of the mixture components varies with changing diffusivity. Indeed, the snapshots in Fig. 2(b) demonstrate that at high D_0 (point D), both mixture components are in a gas state and not segregated; both of these properties prevent a traveling state. Interestingly, the system in Fig. 2(b) at point C does possess one dense and one gaseous phase and is completely segregated between A and B, as shown by a high segregation order parameter $\langle\sigma\rangle$ [32] in Fig. 2(c). Nonetheless, persistently high fluctuations in the distribution of A-particles prevent a traveling state also here: we conclude that segregation into a dense and gaseous phase, even alongside a large nonreciprocity parameter δ , does not by itself guarantee the existence of a traveling phase.

We next study the behavior for moderate D_0 . Here, the blue line in Fig. 2(a) shows an initially surprising intermediate maximum in the mean angular velocity. This is caused by incomplete separation of the mixture within our finite simulation time (see Fig. S3 [32]) at low D_0 when the system is initialized in a mixed state. A system starting in a completely segregated state [dashed line in Fig. 2(a)], on the other hand, has an angular velocity decreasing monotonically with D_0 . Consistently with this picture, the degree of segregation $\langle\sigma\rangle$ of the mixture from a mixed initial state is first facilitated kinetically by increasing D_0 [Fig. 2(c)], until it reaches a maximum. Afterwards, it decreases as both components become gaseous and mix. When initializing in a segregated state, on the other hand [dashed line in Fig. 2(c)], there is no issue in reaching a segregated state kinetically and the degree of segregation decreases essentially monotonically with D_0 .

The dependence of the mean angular velocity on the nonreciprocity parameter δ is rather simpler: monotonically increasing and approximately linear when diffusivity is kept constant ($D_0 = 10^{-3}$). Figure 2(d) shows $\Delta\langle|\omega|\rangle \equiv \langle|\omega|\rangle - \langle|\omega|\rangle_0$; the second term subtracts off the uninteresting fluctuations of ω in the reciprocal case $\delta = 0$. The linearity suggests that the interface between the A and B phases remains largely unaffected by increasing δ , with just the interfacial driving force increasing linearly as the imbalance between AB and BA attractions is proportional to δ .

A phase diagram can be created from the above results by plotting the mean angular velocity as a function of δ and D_0 . In Fig. 2(e) lighter colors correspond to higher $\langle|\omega|\rangle$, i.e., pronounced traveling states (cf. similar results for PBC [32], Figs. S4 and S5). The appearance of a traveling regime at high nonreciprocity and low diffusivity is also found in the predator-prey regime (Fig. S9 [32]) and for larger system sizes (Fig. S11 [32]), and is consistent with earlier studies [15,16,33].

Effect of geometry and dimensionality. Next we study the behavior of traveling states as a function of the geometry and hence (effective) spatial dimension (while keeping density, nonreciprocity and diffusivity fixed). In the annular geometry, we confine our system between two concentric circles of radius R_{in} and R_{out} . For $R_{\text{in}} \simeq R_{\text{out}}$ the system is, up to small corrections from the annulus curvature [32], equivalent to a straight channel (with PBC in the direction of its long axis) as considered in [16], whereas for $R_{\text{in}} = 0$ we have a confined $2d$ system. We observe traveling states [see Fig. 3(a) for snapshots] to be more persistent in the narrow channel

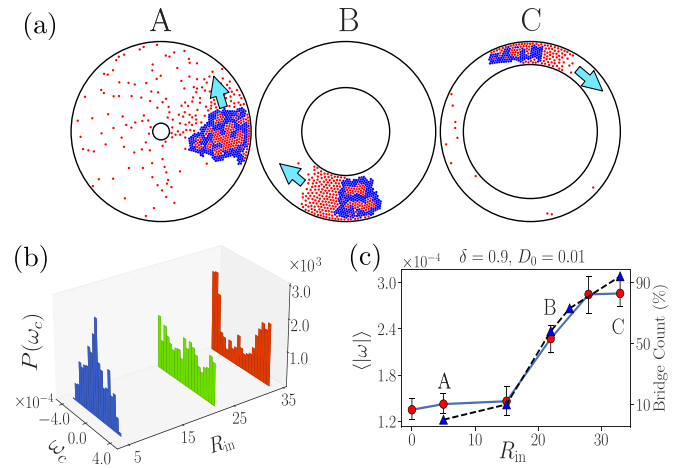


FIG. 3. (a) Typical snapshots of the nonreciprocal binary mixture in an annular geometry (same density $\rho = 0.1$ and outer radius $R_{\text{out}} = 42$ as in Fig. 1, $\delta = 0.9$, $D_0 = 0.01$) for inner radius $R_{\text{in}} = 5$ (A), 22 (B), and 33 (C), respectively. (b) Distribution for the angular velocity of the center of mass ω_c for three different R_{in} , showing clear peaks in the narrow channel regime ($R_{\text{in}} = 33$). (c) Red dots: Average absolute angular velocity $\langle|\omega|\rangle$ as a function of the inner channel radius R_{in} . Blue triangles: Percentage of bridgelike structures, which follows an almost identical trend.

limit while with decreasing R_{in} the motion becomes more erratic (see Fig. S6 for persistence time data and Fig. S7 for the distribution of the linear velocity magnitude [32]). The distribution of the center of mass angular velocity $P(\omega_c)$ shows characteristic peaks at nonzero ω_c (and its negative) at larger values of R_{in} , while it is unimodal for $R_{\text{in}} = 5$ [Fig. 3(b)]. The mean angular velocity also decreases with the inner radius [Fig. 3(c)], indicating that traveling phases become more transient as the effective dimension changes from one to two.

Inspection of Fig. 3(a) suggests that this suppression of traveling states at smaller R_{in} sets in when the traveling solid cluster no longer forms a bridge touching both circular walls. Particles from the gas phase can then “leak” past the cluster (see the movie in the Supplemental Material [32]), causing it to reverse direction. To substantiate this hypothesis we measured the probability for configurations to contain bridges. This bridging probability decreases significantly with the inner radius as indicated by Fig. 3(c) and in fact follows an almost identical trend to $\langle|\omega|\rangle$. It should be noted that our $2d$ ($R_{\text{in}} = 0$) system is confined by a physical wall, which makes it distinct from systems with PBC where clusters can bridge across periodic boundaries [15].

Effects of density. Finally, we study how the overall number density ρ of a nonreciprocal mixture influences the existence of traveling states; Fig. 4(a) shows snapshots at three exemplary ρ , Fig. 4(b) the instantaneous angular density distributions. The mean angular velocity $\langle|\omega|\rangle$ exhibits a non-monotonic response with density [Fig. 4(c)]. This can be rationalized from the fact that a well-defined asymmetric interface between two species only forms at an intermediate density. Indeed, Fig. 4(b) indicates that at low ρ , A and B particles are typically far apart. For moderate ρ , further analysis reveals that the small angular velocities are correlated with

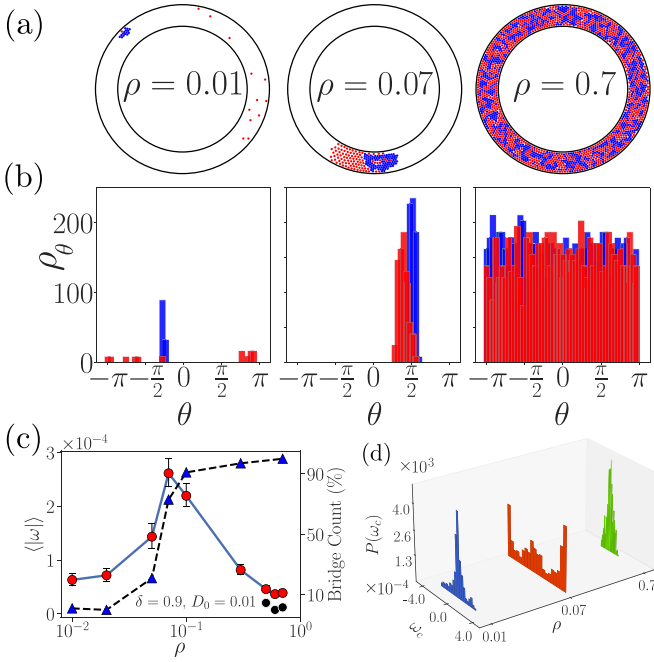


FIG. 4. (a) Snapshots of systems with densities $\rho = 0.01, 0.07, 0.7$ (other parameters as in Fig. 1: $D_0 = 0.01, \delta = 0.9, R_{in} = 33, R_{out} = 42$). (b) Angular distribution of particle number density for the configurations in (a). (c) Red dots: average angular velocity $\langle |\omega| \rangle$ versus density. Black dots: results for a completely segregated, rather than mixed, initial condition. Blue triangles: probability of bridge formation. (d) Distribution of the center of mass angular velocity ω_c , with clear peak demonstrating a traveling state at intermediate ρ .

the bridging probability as before [blue triangles in Fig. 4(c)]: only once a bridge between inner and outer walls exists, will a gas of B particles “pile up” on one side of a traveling A cluster and so form an AB interface there. This behavior is not due to any symmetry breaking between the outer and inner radius, since the correlation between the appearance of bridges and the velocity of the traveling state is also found in a quasi-1D system, cf. Fig. S12 in the SM [32].

For different reasons, the system also loses the asymmetric interface between the two species at high ρ . Starting from a mixed initial state, the high density hinders the segregation kinetics so that A and B particles only form small domains without macroscopic interfaces [see snapshot and angular density for $\rho = 0.7$ in Figs. 4(a) and 4(b)]. Even starting from segregated initial conditions [black points in Fig. 4(c)], however, no traveling state occurs because there is not enough space to create the necessary density gradient of the gaseous B species. With a nearly constant density within the B phase, the two macroscopic interfaces between A and B are then symmetric with each other so that the net unbalanced forces generated at each individual interface cancel. As a result, intermediate densities are optimal for generating traveling states, where the probability distribution of the center of mass angular velocity [Fig. 4(d)] again shows clear peaks at nonzero ω_c .

Finally we combine the data from variation of the inner radius and the density into a second phase diagram (see Fig. 5). The white squares have been obtained by setting a threshold

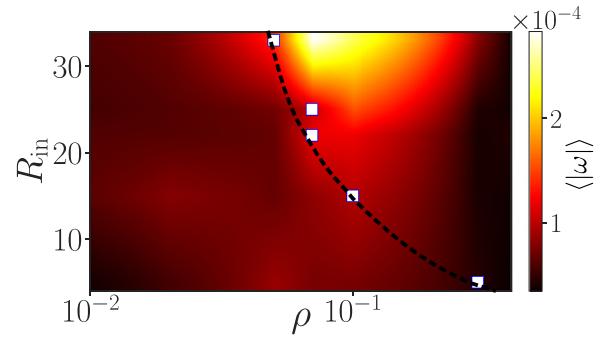


FIG. 5. Phase diagram from heat map of $\langle |\omega| \rangle$ as a function of density ρ and inner radius with $\delta = 0.9, D_0 = 0.01$, and $R_{out} = 42$. White squares: densities ρ where the bridge probability surpasses 20% for each radius. Dashed line: guide to the eye.

on the bridging probability and are seen to demarcate traveling and nontravelling states well in the low density part of the phase diagram. In the high-density region, the difficulty of forming asymmetric interfaces kicks in to prevent the formation of traveling states.

Summarizing, we have studied the emergence and robustness of traveling states in a nonreciprocal binary particle mixture. We find that such states, with an appreciable velocity, appear in the low nonreciprocity regime only when a “chasing” cluster with a solidlike structure is present. The traveling velocity increases with increasing degree of nonreciprocity and with decreasing diffusivity, because of stronger segregation between the phases. Varying the system geometry, traveling states become more persistent as we move from a (confined) two-dimensional scenario to an effectively one-dimensional annulus, where the solid cluster can form a bridge between inner and outer walls. This effect also facilitates traveling states at intermediate density and prevents them for dilute systems; high density also suppresses traveling states because asymmetric interfaces can no longer form. Thus, traveling states may only be found in a narrow region of the parameter space, where the conditions for their appearance are optimal. We have also found that most of our conclusions hold for the predator-prey regime ($\delta > 1$) and for larger system sizes (as detailed in the SM [32]), although further studies are required in order to ascertain the validity of our conclusions in the thermodynamic limit.

Our results should be amenable to verification in experiments on nonreciprocal particle systems [34,35]. Our identification of the physical mechanisms generating traveling states will also be of broader importance for understanding the behavior of nonreciprocal phase separating mixtures and nonequilibrium pattern formation more generally, including—outside of physics—in, e.g., prey-predator models.

Acknowledgments. This project has received funding from the European Union’s Horizon 2020 research and innovation programme under the Marie Skłodowska-Curie Grant Agreement No. 893128. Simulations were run on the Goe-Grid cluster at the University of Göttingen, which is supported by the Deutsche Forschungsgemeinschaft (Projects ID 436382789 and ID 493420525).

R.M. and S.S.J. contributed equally to this work.

- [1] S. Asakura and F. Oosawa, On interaction between two bodies immersed in a solution of macromolecules, *J. Chem. Phys.* **22**, 1255 (1954).
- [2] T. Emig, N. Graham, R. L. Jaffe, and M. Kardar, Casimir forces between arbitrary compact objects, *Phys. Rev. Lett.* **99**, 170403 (2007).
- [3] A. V. Ivlev, J. Bartnick, M. Heinen, C.-R. Du, V. Nosenko, and H. Löwen, Statistical mechanics where Newton's third law is broken, *Phys. Rev. X* **5**, 011035 (2015).
- [4] J. P. Banerjee, R. Mandal, D. S. Banerjee, S. Thutupalli, and M. Rao, Unjamming and emergent nonreciprocity in active ploughing through a compressible viscoelastic fluid, *Nat. Commun.* **13**, 4533 (2022).
- [5] R. K. Gupta, R. Kant, H. Soni, A. K. Sood, and S. Ramaswamy, Active nonreciprocal attraction between motile particles in an elastic medium, *Phys. Rev. E* **105**, 064602 (2022).
- [6] J. Dzubiella, H. Löwen, and C. N. Likos, Depletion forces in nonequilibrium, *Phys. Rev. Lett.* **91**, 248301 (2003).
- [7] J. Bartnick, M. Heinen, A. V. Ivlev, and H. Löwen, Structural correlations in diffusiophoretic colloidal mixtures with non-reciprocal interactions, *J. Phys.: Condens. Matter* **28**, 025102 (2016).
- [8] E. A. Lisin, O. S. Vaulina, and O. F. Petrov, Verifying the reciprocity of interparticle interaction forces in strongly coupled systems, *J. Exp. Theor. Phys.* **124**, 678 (2017).
- [9] N. P. Kryuchkov, A. V. Ivlev, and S. O. Yurchenko, Dissipative phase transitions in systems with nonreciprocal effective interactions, *Soft Matter* **14**, 9720 (2018).
- [10] Y.-F. Lin, A. Ivlev, H. Löwen, L. Hong, and C.-R. Du, Structure and dynamics of a glass-forming binary complex plasma with non-reciprocal interaction, *Europhys. Lett.* **123**, 35001 (2018).
- [11] S. A. M. Loos, S. M. Hermann, and S. H. L. Klapp, Non-reciprocal hidden degrees of freedom: A unifying perspective on memory, feedback, and activity, [arXiv:1910.08372](https://arxiv.org/abs/1910.08372).
- [12] N. P. Kryuchkov, L. A. Mistryukova, A. V. Sapelkin, and S. O. Yurchenko, Strange attractors induced by melting in systems with nonreciprocal effective interactions, *Phys. Rev. E* **101**, 063205 (2020).
- [13] L. P. Dadhichi, J. Kethapelli, R. Chajwa, S. Ramaswamy, and A. Maitra, Nonmutual torques and the unimportance of motility for long-range order in two-dimensional flocks, *Phys. Rev. E* **101**, 052601 (2020).
- [14] P. R. N. Falcão and M. L. Lyra, Rectification of acoustic phonons in harmonic chains with nonreciprocal spring defects, *J. Phys.: Condens. Matter* **32**, 245401 (2020).
- [15] S. Saha, J. Agudo-Canalejo, and R. Golestanian, Scalar active mixtures: The nonreciprocal Cahn-Hilliard model, *Phys. Rev. X* **10**, 041009 (2020).
- [16] Z. You, A. Baskaran, and M. C. Marchetti, Nonreciprocity as a generic route to traveling states, *Proc. Natl. Acad. Sci. USA* **117**, 19767 (2020).
- [17] S. A. M. Loos and S. H. L. Klapp, Irreversibility, heat and information flows induced by non-reciprocal interactions, *New J. Phys.* **22**, 123051 (2020).
- [18] M. Fruchart, R. Hanai, P. B. Littlewood, and V. Vitelli, Non-reciprocal phase transitions, *Nature* **592**, 363 (2021).
- [19] T. Carletti and R. Muolo, Non-reciprocal interactions enhance heterogeneity, *Chaos, Solitons & Fractals* **164**, 112638 (2022).
- [20] Z. Zhang and R. Garcia-Millan, Entropy production of non-reciprocal interactions, [arXiv:2209.09721](https://arxiv.org/abs/2209.09721).
- [21] C. Packard and D. M. Sussman, Non-reciprocal forces and exceptional phase transitions in metric and topological flocks, [arXiv:2208.09461](https://arxiv.org/abs/2208.09461).
- [22] J. Agudo-Canalejo and R. Golestanian, Active phase separation in mixtures of chemically interacting particles, *Phys. Rev. Lett.* **123**, 018101 (2019).
- [23] K. L. Kreienkamp and S. H. L. Klapp, Clustering and flocking of repulsive chiral active particles with non-reciprocal couplings, *New J. Phys.* **24**, 123009 (2022).
- [24] T. Frohoff-Hülsmann, J. Wrembel, and U. Thiele, Suppression of coarsening and emergence of oscillatory behavior in a Cahn-Hilliard model with nonvariational coupling, *Phys. Rev. E* **103**, 042602 (2021).
- [25] T. Frohoff-Hülsmann and U. Thiele, Localized states in coupled Cahn-Hilliard equations, *IMA J. Appl. Math.* **86**, 924 (2021).
- [26] F. Brauns and M. C. Marchetti, Non-reciprocal pattern formation of conserved fields, *Phys. Rev. X* **14**, 021014 (2024).
- [27] T. Frohoff-Hülsmann and U. Thiele, Nonreciprocal Cahn-Hilliard model emerges as a universal amplitude equation, *Phys. Rev. Lett.* **131**, 107201 (2023).
- [28] H. Alston, L. Cocconi, and T. Bertrand, Irreversibility across a nonreciprocal PT -symmetry-breaking phase transition, *Phys. Rev. Lett.* **131**, 258301 (2023).
- [29] T. Suchanek, K. Kroy, and S. A. M. Loos, Entropy production in the nonreciprocal Cahn-Hilliard model, *Phys. Rev. E* **108**, 064610 (2023).
- [30] Y. Duan, J. Agudo-Canalejo, R. Golestanian, and B. Mahault, Dynamical pattern formation without self-attraction in quorum-sensing active matter: The interplay between nonreciprocity and motility, *Phys. Rev. Lett.* **131**, 148301 (2023).
- [31] A. Dinelli, J. O'Byrne, A. Curatolo, Y. Zhao, P. Sollich, and J. Tailleur, Self-organization of bacterial mixtures in the presence of quorum-sensing interactions, *Nat. Commun.* **14**, 7035 (2023).
- [32] See Supplemental Material at <http://link.aps.org/supplemental/10.1103/PhysRevE.109.L062602> for robustness of travelling states in generic nonreciprocal mixtures, which includes Refs. [36–44].
- [33] J. Bartnick, A. Kaiser, H. Löwen, and A. V. Ivlev, Emerging activity in bilayered dispersions with wake-mediated interactions, *J. Chem. Phys.* **144**, 224901 (2016).
- [34] R. Niu, A. Fischer, T. Palberg, and T. Speck, Dynamics of binary active clusters driven by ion-exchange particles, *ACS Nano* **12**, 10932 (2018).
- [35] C. H. Meredith, P. G. Moerman, J. Groenewold, Y.-J. Chiu, W. K. Kegel, A. van Blaaderen, and L. D. Zarzar, Predator-prey interactions between droplets driven by non-reciprocal oil exchange, *Nat. Chem.* **12**, 1136 (2020).
- [36] J. Buhl, D. J. T. Sumpter, I. D. Couzin, J. J. Hale, E. Despland, E. R. Miller, and S. J. Simpson, From disorder to order in marching locusts, *Science* **312**, 1402 (2006).
- [37] A. Bricard, J.-B. Caussin, N. Desreumaux, O. Dauchot, and D. Bartolo, Emergence of macroscopic directed motion in populations of motile colloids, *Nature (London)* **503**, 95 (2013).
- [38] D. J. G. Pearce and M. S. Turner, Emergent behavioural phenotypes of swarming models revealed by mimicking a frustrated anti-ferromagnet, *J. R. Soci. Interface* **12**, 20150520 (2015).

- [39] C. Joshi, Z. Zarei, M. M. Norton, S. Fraden, A. Baskaran, and M. F. Hagan, From disks to channels: Dynamics of active nematics confined to an annulus, *Soft Matter* **19**, 5630 (2023).
- [40] A. Souslov, B. C. van Zuiden, D. Bartolo, and V. Vitelli, Topological sound in active-liquid metamaterials, *Nat. Phys.* **13**, 1091 (2017).
- [41] D. Geyer, D. Martin, J. Tailleur, and D. Bartolo, Freezing a flock: Motility-induced phase separation in polar active liquids, *Phys. Rev. X* **9**, 031043 (2019).
- [42] A. Kolpas, J. Moehlis, and I. G. Kevrekidis, Coarse-grained analysis of stochasticity-induced switching between collective motion states, *Proc. Natl. Acad. Sci. USA* **104**, 5931 (2007).
- [43] E. M. Lennon, G. O. Mohler, H. D. Ceniceros, C. J. García-Cervera, and G. H. Fredrickson, Numerical solutions of the complex Langevin equations in polymer field theory, *Multiscale Modeling & Simulation* **6**, 1347 (2008).
- [44] R. Brito and R. Soto, Competition of Brazil nut effect, buoyancy, and inelasticity induced segregation in a granular mixture, *Eur. Phys. J. Spec. Top.* **179**, 207 (2009).